

## Tuning Polymer Crystallinity

Kiriaki Chrissopoulou<sup>1</sup>, Hellen Papananou<sup>1,2</sup>, Elena Perivolari<sup>1,3</sup> and Spiros H. Anastasiadis<sup>1,2</sup>

<sup>1</sup>Institute of Electronic Structure and Laser, Foundation for Research and Technology-Hellas,  
Heraklion Crete, Greece

<sup>2</sup>Department of Chemistry, University of Crete, Heraklion Crete, Greece

<sup>3</sup>Department of Materials Science, University of Crete, Heraklion Crete, Greece

Email: [kiki@iesl.forth.gr](mailto:kiki@iesl.forth.gr)

**Keywords:** Polymer Crystallization, Confinement, Poly (ethylene oxide), Silica nanoparticles

### Abstract

Addition of nanosized inorganic materials in a polymeric matrix results to nanohybrids with optimized properties with respect to the initial components. On the other hand, the behavior of polymers when they are restricted in space or when they are close to surfaces can be very different from that in the bulk.

Controlling the crystallization behavior of semi-crystalline polymers is of paramount importance since it largely determines their final properties. A way to affect crystallinity is via the addition of nanosized additives in the polymer matrix that are usually utilized to improve the polymer properties. In the present work, we demonstrate the control of the degree of polymer crystallinity in poly(ethylene oxide), PEO, nanohybrids when layered silicates with galleries of ~1nm or when nanoparticles of different sizes, i.e., smaller, comparable and larger than the polymer radius of gyration are utilized as additives. This way a varying degree of chain confinement is introduced.

### 1. Introduction

Polymer nanocomposites, comprised of a polymer matrix and inorganic or carbon additives (e.g., nanoparticles, nanotubes, clays, graphene, etc.) as the nanofiller, possess improved and often innovative physicochemical properties compared to conventionally filled systems.[1-4] On the other hand polymer crystallization has been attracting the scientific interest because of the hierarchical nano/meso/macro-scopic morphologies formed and because it determines to a large extend the final material properties; its understanding can provide an effective way for the prediction of thermal, mechanical, electrical and transport properties and, thus, allows the use of the proper semi-crystalline polymer in novel applications.[5] Polymer crystallization is strongly influenced by the presence of additives and/or surfaces, whereas, confinement may drive the polymers to crystallize within spaces that are of the same order of magnitude as individual lamellar crystals in the bulk. The way polymers crystallize under confinement and/or close to surfaces is a fundamental problem and, at the same time, it has a significant importance for technological applications.[6] It comes out that of particular importance in the study of crystallization of polymers filled with nanoparticles is the size and the shape of the nanoparticle, the filler loading, the dispersion of the nanoparticles within the matrix as well as the polymer size and the nature of the interactions between the polymer and the nanoparticle, with the latter two influencing the surface adsorption as well.

A highly crystalline polymer, which is utilized in a broad range of technological applications, is poly(ethylene oxide), PEO. Its hydrophilicity, biocompatibility, versatility and high ion transport properties makes it suitable for many fields of research including biomaterials, drug-delivery and solid state polymer electrolytes.[7,8] Various methods have been proposed, over the years, to increase the

volume fraction of its amorphous phase and to improve its conductivity at ambient temperatures; a promising way to influence polymer crystallinity is the incorporation of nanoparticles, creating a nanocomposite.[9]

It is, therefore, evident that achieving control of polymer crystallization is of critical importance. In that respect, we utilize PEO/silicate [10] (Na<sup>+</sup>-MMT) and PEO/silica [11] nanohybrids with nanoparticles with sizes smaller (NP<sub>7</sub>), comparable (NP<sub>18.5</sub>) and larger (NP<sub>67</sub>) than the PEO radius of gyration over an extended range of compositions from pure polymer to the highest possible, thus varying the interfacial area and the degree of polymer confinement. This study contributes to a deeper understanding of the crystallization process close to inorganic surfaces.

## 2. Experimental Section

### 2.1. Materials

Poly(ethylene oxide) homopolymer, PEO, was purchased from Aldrich. Its molecular weight  $M_V$  is 100.000 g/mol and its polydispersity index is  $M_w/M_n = 2.4$ , as determined by size exclusion chromatography utilizing polystyrene standards. The polymer possesses hydroxyl chain end groups. It exhibits a glass transition temperature  $T_g = -67$  °C and a melting temperature  $T_m = 65.5$  °C. The layered silicate utilized was a hydrophilic sodium montmorillonite, Na<sup>+</sup>-MMT (Southern Clay). The silica nanoparticles used, Ludox LS, Ludox AS40 (Sigma Aldrich) and Nissan Snowtex ZL, were purchased in aqueous dispersions. The nanoparticles possess hydroxyl surface groups, as well.

PEO/Na<sup>+</sup>-MMT nanohybrids were synthesized from melt intercalation whereas the PEO/SiO<sub>2</sub> nanocomposites via solution mixing. Initially, a PEO/water solution was prepared and, then, the appropriate aqueous dispersion of the nanoparticles was added. In all cases the nanocomposites were annealed at 100°C for 1h and subsequently cooled to room temperature at a rate of 10°C/min, to ensure equilibrium.

### 2.2. Experimental Techniques

*Dynamic Light Scattering (DLS)*. For the Dynamic Light Scattering measurements a Brookhaven BI200SM apparatus equipped with a Brookhaven Mini – L30 laser with  $\lambda = 637$  nm was utilized. All dispersions were diluted with nanopure water down to 0.1% concentration. Filtering of the samples in dust-free light scattering cells was performed using hydrophilic filters with pore size 0.2  $\mu\text{m}$ . All measurements were performed at  $T = 25$ °C in scattering angles covering the range from 30° to 150°. The measured quantity was the autocorrelation function of the scattered intensity that is connected with the corresponding one of the electric field; the latter was analyzed with a K.W.W. function to provide the relaxation time and the scatterer size.

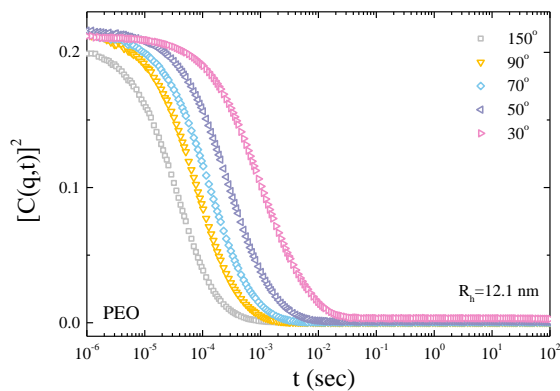
*X-Ray Diffraction (XRD)*. The structural and morphological characterization of the pure materials and of the nanocomposites was performed with X-ray diffraction, using a RINT-2000 Rigaku diffractometer. The X-rays are produced by a 12 kW rotating anode generator with a Cu anode equipped with a secondary pyrolytic graphite monochromator. The Cu K $\alpha$  radiation was used with wavelength  $\lambda = \lambda_{\text{CuK}\alpha} = 1.54$  Å. Measurements were performed for  $2\theta$  from 1.5° to 30° with step of 0.02°.

*Differential Scanning Calorimetry (DSC)*. The thermal properties of the nanocomposites as well as of the bulk polymer were measured with a PL-DSC (Polymer Laboratories) differential scanning calorimeter. The range of temperatures covered was between -100°C and 100°C with a heating/cooling rate of 10°C/min, whereas two heating/cooling cycles were performed in all cases. The melting,  $T_m$ , and crystallization,  $T_c$ , temperatures were obtained from the second cycle to ensure elimination of the effects of thermal history. The heat of fusion of each specimen is obtained when the integral under the melting peak in the measured heat flow curve is divided by the polymer mass and by the heating rate; the degree of crystallinity can be calculated by dividing the heat of fusion with the respective heat of fusion of a 100% crystalline PEO ( $\Delta H_{\text{cryst}} = 196.4$  J/g). Controlled cooling was achieved using liquid

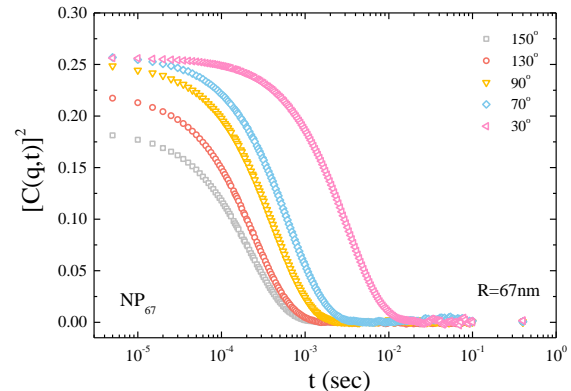
nitrogen and all the measurements were performed under nitrogen flow to prevent the decomposition of the samples.

### 3. Results and Discussion

Figure 1 shows DLS measurements for the PEO polymer (Fig. 1a) and for the large nanoparticles (Fig. 1b). For PEO, the autocorrelation functions showed one main relaxation process with exponential decay ( $\beta_{KWW}=0.95-0.97$ ) that corresponds to a population with hydrodynamic radius  $R_h=12.1$ nm and a very small slower process that was necessary to fit the data. For a polymer coil in theta-conditions this  $R_h$  would indicate a radius of gyration of  $R_g\sim 15.3$ nm. Fig.1b shows the autocorrelation functions of the scattered intensity for a dilute dispersion of the ZL nanoparticles at different scattering angles. In all cases the curves decay as single exponentials ( $\beta_{KWW}=0.98-1.02$ ) and from their relaxation time a size of  $R_{ZL}=67$ nm can be calculated. The situation was very similar for the case of the other two kind of nanoparticles as well and their size were measured as  $R_{LS}=7$ nm and  $R_{AS40}=18.5$ nm; in the following the nanoparticles are denoted as NP<sub>7</sub>, NP<sub>18.5</sub> and NP<sub>67</sub>. Measurement of the size of the nanoparticles by transmission electron microscopy, TEM, was in very good agreement with the DLS results.



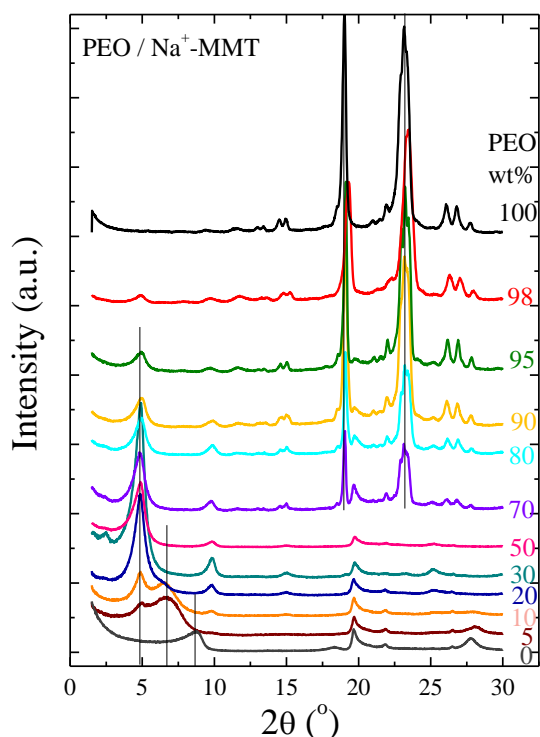
**Figure 1a:** Intensity correlation functions of PEO / water solution at 0.1wt% PEO for different scattering angles.



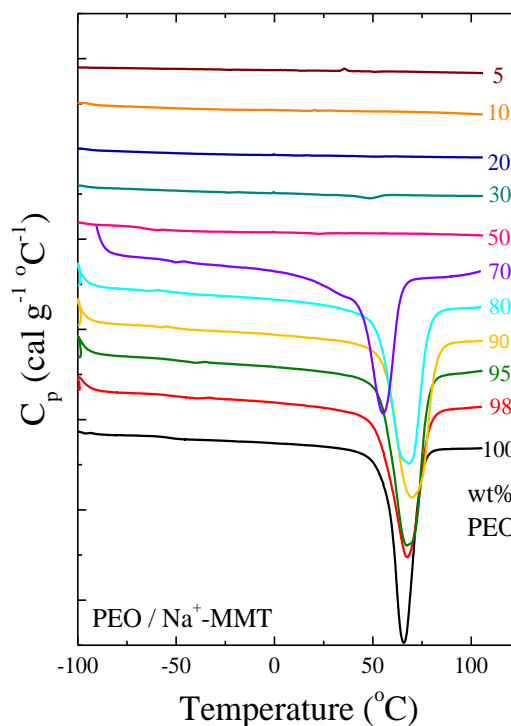
**Figure 1b:** Intensity correlation functions of NP<sub>67</sub> / water dispersion at 0.1wt% NP<sub>67</sub> for different scattering angles.

Figure 2a shows the X-ray diffraction patterns of PEO, Na<sup>+</sup>-MMT and of PEO / Na<sup>+</sup>-MMT nanocomposites with varying polymer concentration. Pure Na<sup>+</sup>-MMT exhibits a main (001) diffraction peak at  $2\theta=8.8^\circ$ , which corresponds to an interlayer distance of 1.0 nm. Upon addition of only 5 wt% PEO, this peak disappears and two other peaks emerge at  $2\theta = 6.7^\circ$  and  $2\theta = 4.8^\circ$ , corresponding to interlayer distances of 1.30 nm and 1.85 nm respectively. The appearance of those peaks indicates that PEO chains have intercalated between the inorganic layers, forming mono- and bi-layers of polymer chains within the interlayer galleries. As PEO concentration increases up to 20 wt%, the relative intensities of the two peaks change; the one corresponding to  $d = 1.85$  nm increases, indicating the formation of more bi-layer filled galleries, while the intensity of the first peak decreases. By further increasing the PEO concentration to 30 and 50 wt%, only bi-layers of intercalated PEO chains are observed as evidenced by the XRD peak at  $2\theta = 4.8^\circ$  which is the only one observed in the low  $2\theta$  range. Equally important, the diffractograms of the nanocomposites show peaks that correspond to those of crystalline PEO only for polymer concentrations 70 wt% and higher. Their absence from the XRD patterns of the nanocomposites with lower PEO content indicates that the intercalated polymer as well as the chains that are in close proximity to the inorganic surfaces are amorphous; it is only the excess polymer outside the completely filled galleries and away from the outside walls of the inorganic particles (in the hybrids with high concentration) that is able to crystallize. It is noted, that a

similar series of nanocomposites that was prepared utilizing solution intercalation gave exactly the same results, thus certifying the attainment of equilibrium in both cases.



**Figure 2a:** X-ray diffractograms of pure PEO (top), Na<sup>+</sup>-MMT (bottom) and PEO / Na<sup>+</sup>-MMT nanocomposites with varying polymer content. The curves have been shifted vertically for clarity.



**Figure 2b:** DSC thermograms (shown in units of heat capacity) of PEO and PEO / Na<sup>+</sup>-MMT nanocomposites with varying polymer content; the data are shown for the second heating. The curves have been shifted vertically for clarity.

These results are further verified by DSC measurements that are shown in Figure 2b; a melting endotherm is observed only for high polymer concentrations. In all cases the measured heat flow is shown normalized with the polymer mass of the nanocomposite and the heating rate so that the integral under the melting curve will directly provide the heat of fusion,  $\Delta H_{\text{exp}}$ . It is obvious that only nanocomposites with polymer content 70wt% or higher exhibit a melting transition (and the respective crystallization), whereas hybrids with lower polymer content are completely amorphous in perfect agreement with the XRD results. The degree of crystallinity of the hybrids can be calculated as % Crystallinity =  $\Delta H_{\text{exp}}/\Delta H_{\text{cryst}}$ , where  $\Delta H_{\text{exp}}$  the measured heat of fusion of the polymer in the nanocomposite and  $\Delta H_{\text{cryst}}=196.4\text{J/g}$  the heat of fusion of a totally crystalline poly(ethylene oxide); this calculation results in that for hybrids with more than 70wt% PEO, the polymer shows an almost constant crystallinity of ~80% whereas the crystallinity drops abruptly to zero for lower compositions.

There is a significant change in the thermal behavior and more specifically in the crystallinity of PEO when nanocomposites with a different additive are investigated, i.e. if the layered silicates are replaced by spherical silica nanoparticles of different sizes. This way the effect of the confinement on polymer crystallization can be studied. Figure 3a shows X-ray diffractograms of PEO / SiO<sub>2</sub> nanohybrids containing 50wt% of PEO and 50wt% of NP<sub>7</sub>, NP<sub>18.5</sub> and NP<sub>67</sub>. It is clear that the morphology of the polymer is completely different compared to the one of the same concentration with the layered silicates as the additive. In the current case, well defined peaks at similar diffraction angles with the peaks of the crystalline PEO are observed in contrast with their complete absence in the diffractogram of 50wt% PEO / 50wt% Na<sup>+</sup>-MMT. Differences exist though when someone compares quantitatively

the measurements for the three different nanoparticles and higher crystallinity is observed for the hybrid with the larger nanoparticles.

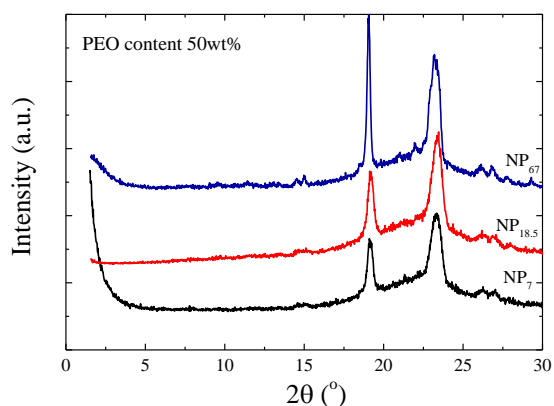


**Figure 3a:** X-ray diffractograms of PEO / SiO<sub>2</sub> nanohybrids with three different sizes of nanoparticles. The curves have been shifted vertically for clarity.

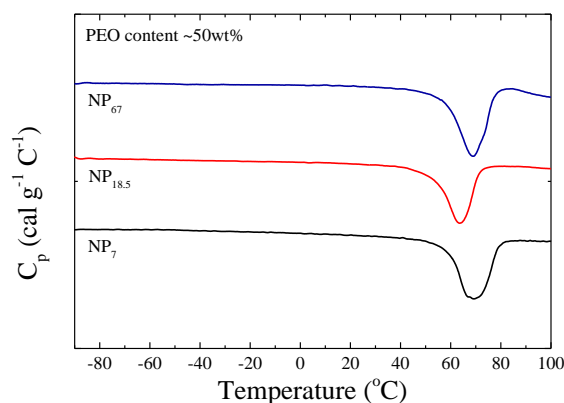


**Figure 3b:** DSC thermograms of PEO / SiO<sub>2</sub> nanohybrids with three different sizes of nanoparticles; the data are shown for the second heating. The curves are shifted vertically for clarity.

The DSC measurements of the three nanohybrids with 50wt% PEO and the different silica nanoparticles are shown in Figure 3b. It is clear that all three thermograms show a melting transition. The melting temperatures that the transition is observed are  $T_{m,7}=69.5^{\circ}\text{C}$  for the hybrids with NP<sub>7</sub>,  $T_{m,18.5}=63.5^{\circ}\text{C}$  for the hybrids with NP<sub>18.5</sub> and  $T_{m,67}=68.5^{\circ}\text{C}$  for the hybrids with NP<sub>67</sub>. It is noted that the melting temperature for the pure polymer is  $T_m=65.5^{\circ}\text{C}$ . The degree of crystallinity, in all cases, can be calculated by dividing the heat of fusion, obtained from the integral under the peak of the specific peak, with the respective heat of fusion of a 100% crystalline PEO ( $\Delta H_{\text{crys}}=196.4 \text{ J/g}$ ). It comes out that the crystallinity for the hybrids with NP<sub>67</sub> is  $X_{67}\sim 75\%$ , with NP<sub>18.5</sub> is  $X_{18.5}\sim 64\%$  and with NP<sub>7</sub> is  $X_7\sim 63\%$ . It is reminded that in the case of the nanohybrids with layered silicates, the polymer was purely amorphous and thus its crystallinity is  $X=0$ . It is clear that in the latter case and for the specific polymer concentration, the polymer is significantly confined since the majority of the chains are intercalated within the galleries of the clay particle whereas the rest are adsorbed around its outer surfaces. Moreover, when the nanohybrids with the silica nanoparticles are considered, it is clear that for a constant volume fraction the degree of confinement increases as the size of the nanoparticle decreases since their number increases and thus the interparticle distance decreases. So, it can be concluded that increase of the degree of confinement affects significantly the chain morphology and causes a decrease of the degree of crystallinity.

#### 4. Conclusions

Poly(ethylene oxide) with  $R_h\sim 12\text{nm}$  was used as the matrix for nanocomposites with either layered silicates or silica nanoparticles of radii 7, 18.5 and 67nm, as additives. In all cases, the degree of crystallinity of the polymer is almost constant as the inorganic additives are introduced whereas it begins decreasing below a certain characteristic concentration of nanoadditives; this concentration is the highest in the case of the clay particles whereas it depends on the size of the nanoparticles when it comes to the silica. The behavior is attributed to chains crystallizing under confinement, close to the nanoparticles or in the space between them. The polymer chains suffer the most intense confinement effects in the case of the layered silicates followed by the small nanoparticles, since these provide larger inorganic surface area and larger degree of confinement for the same polymer content.

## Acknowledgments

This work was performed in the framework of PROENYL research project, Action KRIPIS, project MIS-448305 (2013SE01380034), funded by the General Secretariat for Research and Technology, Ministry of Education, Greece and the European Regional Development Fund (Sectoral Operational Programme: Competitiveness and Entrepreneurship, NSRF 2007-2013) and by the NFFA Europe project of the European Union (grant agreement No. 654360).

## References

- [1] D. Schmidt, D. Shah, E. P. Giannelis. *Curr. Opin. Sol. Stat. Mater. Sci.* 6:205-212, 2002.
- [2] A. Bansal, H. Yang, C. Li, K. Cho, B. C. Benicewicz, S. K. Kumar, L. S. Schadler. *Nature Mater.* 4:693-698, 2005.
- [3] R. J. Tseng, C. Tsai, L. Ma, J. Ouyang, C. S. Ozkan, Y. Yang. *Nature Nano* 1:72-77, 2006.
- [4] P. Akcora, H. Liu, S. K. Kumar, J. Moll, Y. Li, B. C. Benicewicz, L. S. Schadler, D. Acehan, A. Z. Panagiotopoulos, V. Pryamitsyn, V. Ganesan, J. Ilavsky, P. Thiyagarajan, R. H. Colby, J. F. Douglas. *Nature Mater.* 8:354-359, 2009.
- [5] G. Reiter. *Polymer Crystallization: Observations, Concepts and Interpretations*. Springer Berlin Heidelberg, 2010.
- [6] R. M. Michell, A. J Müller. *Prog. Polym. Sci.* 54-55:183-213, 2016.
- [7] A. A. Teran, M. H. Tang, S. A. Mullin, N. P. Balsara. *Sol. Stat. Ion.* 203:18-21, 2011.
- [8] X. S. Fan, Z. G. Hu, G. W. Wang. *RSC Adv.* 5:100816-100823, 2015.
- [9] A. Kellarakis, E. P. Giannelis. *Polymer* 52:2221-2227, 2011.
- [10] K. Chrissopoulou, K. S. Andrikopoulos, S. Fotiadou, S. Bollas, C. Karageorgaki, D. Christofilos, G. A. Voyiatzis, S. H. Anastasiadis. *Macromolecules* 44:9710-9722, 2011.
- [11] H. Papananou, E. Perivolari, K. Chrissopoulou, S. H. Anastasiadis. *submitted* 2018.